# Effects of thermally activated hole escape mechanism on the optical and electrical properties in *p*-type Si $\delta$-doped GaAs(311)*A* layers

M. Frizzarini, E. C. F. da Silva, A. A. Quivy, A. Cavalheiro, and J. R. Leite
*Instituto de Física da Universidade de São Paulo, CP 66318, 05315-970 São Paulo, SP, Brazil*

E. A. Meneses
*Instituto de Física Gleb Wataghin, Universidade Estadual de Campinas, CP 6165, 17083-970 Campinas, SP, Brazil*

(Received 24 August 1999; revised manuscript received 7 December 1999)

A series of periodically spaced *p*-type $\delta$-doped GaAs(311)*A* layers, with a doping period varying from 100 to 500 Å, was investigated by Hall effect and photoluminescence measurements in the range of 2 up to 280 K. An enhancement of the Hall mobility by a factor of 5 was observed around 100 K for the structure with the largest period with respect to the one with the smallest period. Photoluminescence measurements carried out at different temperatures revealed that the physical origin of the mobility enhancement was related to the escape of confined holes from the two-dimensional hole gas to the undoped GaAs region between $\delta$-doped layers. Both optical and transport data provided strong evidence of the two-dimensional to three-dimensional transition related to the change from isolated $\delta$ wells to a superlattice of $\delta$ wells characterized by the formation of minibands.

## I. INTRODUCTION

Delta-doped ($\delta$-doped) semiconductor materials have attracted the attention of many researchers since it was demonstrated that they could be very important to the development of high-performance devices.[1,2] From a fundamental point of view, $\delta$-doped layers provide interesting systems for studying the fundamental properties of a two-dimensional carrier gas in the limit of strong coupling with the ionized impurities of the $\delta$-doped layers. Although several theoretical and experimental works have already been devoted to the study of the fundamental properties of single,[3–5] double,[6,7] and multiple $\delta$-doped (M$\delta$D) layers,[8–20] in GaAs most of them were related to *n*-type $\delta$-doped layers. Little is known about the relevant mechanisms that limit the mobility of the two-dimensional hole gas (2DHG), as well as which ones control its temperature dependence in *p*-type M$\delta$D GaAs layers.

M$\delta$D layers are systems with a periodic sequence of equally spaced $\delta$-doped layers of the same doping type and level, separated by undoped regions of the host material. When the coupling of the majority-carrier wave functions between adjacent $\delta$ wells replaces the characteristic discrete energy-level scheme of an isolated $\delta$ well by a set of minibands of finite width, the structure is referred to as a $\delta$-doped superlattice ($\delta$DSL). Self-consistent calculations and experimental results about the miniband formation (change from a 2D to 3D behavior, i.e., from M$\delta$D layers to a $\delta$DSL) have already been reported for *n*-type $\delta$-doped GaAs structures.[15,16]

In the present work, we report on a detailed temperature-dependence investigation of the Hall mobility and of the optical properties in periodically spaced multiple *p*-type $\delta$-doped GaAs layers. A set of samples with a fixed nominal acceptor concentration $N_A$ in the $\delta$-doped layers but with different doping periods $d$ (100 Å$\leqslant d \leqslant$500 Å) was investigated. In our experiments, we observed that the Hall mobility monotonically increased for raising temperature between 40 and 100 K. This increase of the mobility is more pronounced for the structures with the largest periods. For $T>100$ K, the mobility is mainly limited by optical-phonon scattering. The analysis of our results indicates that the behavior of the Hall mobility as a function of temperature in the range from 40 up to 100 K is related to the escape of confined holes from the 2DHG to the undoped GaAs region between adjacent $\delta$-doped layers. This interpretation is confirmed by the analysis of the intensity of the emissions observed in our photoluminescence (PL) spectra as a function of temperature.

## II. SAMPLE PREPARATION

The samples analyzed here were grown in a Gen II Mod. MBE system from Varian on top of ‘‘epi-ready’’ semi-insulating GaAs(311)*A* substrates from American Crystal Technology (AXT). Under specific growth conditions,[21] the Si dopant can enter the As sites of the (311)*A* surface, leading to the *p*-type character of the GaAs layer. This is generally possible when the V/III flux ratio is kept as low as possible (below 4) and the growth temperature is above 450 °C, to be sure that some As deficiency will be generated at the surface and will favor the incorporation of Si atoms into the As sublattice. However, the As flux must be large enough in order to keep the $2\times4$ surface reconstruction during growth and ensure a good morphological quality of the films.[22] The planar doping was achieved by the standard growth-interruption technique and simultaneous evaporation of the dopant. After a degas in the entry/exit and buffer chamber, the substrates were transferred individually into the growth chamber for oxide desorption around 580 °C under an $As_4$ flux and degassed at 630 °C for 5 min. The removal of the oxide layer was monitored using the RHEED (reflection high-energy electron-diffraction) pattern that switched from diffuse to spotty. This transition was also used to check the calibration of the infrared pyrometer, which was monitoring the sample temperature during the growth. All the samples were grown with a V/III flux ratio of 3 and had the same basic configuration: a 1-$\mu$m-thick GaAs buffer layer followed by a periodic Si $\delta$-doped structure and finally a 300-Å -thick GaAs cap layer. The periodic structure consisted of 30 Si $\delta$-doped planes, with a fixed nominal sheet concentration $N_A = 1.5\times10^{13}$ cm$^{-2}$, separated by the same distance. The buffer layer was grown at 580 °C and the rest of the structure at 500 °C to avoid diffusion of the dopant into the host material that could yield a broadening of the doping profile. The growth was interrupted during 30 sec before the deposition of each Si layer in order to smooth the surface. Five samples were grown with different periods and designated as S500, S300, S250, S200, and S100. The number indicates the distance (Å) between two adjacent doping planes.

## III. EXPERIMENTAL DETAILS

The transport measurements were carried out in a superconducting magnet using the standard van der Pauw configuration. The linearity of the $I\times V$ curves was a proof of the good quality of the Ohmic contacts that were made using an In-Zn alloy. In order to get accurate and reliable data for the mobility, each mobility value presented in this work was actually resulting from a magnetoresistance curve of 400 data points obtained by sweeping the magnetic field between $-0.5$ T and 0.5 T (back and forth). The data were taken in the constant-current mode, with a current of 100 $\mu$A, and the contacts were permutated, although no significant anisotropy was observed. Photoluminescence (PL) measurements were performed in an optical helium-bath cryostat with variable-temperature facilities. The samples were excited with the 5145 Å line of an argon-ion laser at a power density of 60 W/cm$^2$. The luminescence signal was dispersed by a 0.75 m monochromator, detected by a S1 photomultiplier, and the electrical signal was amplified and processed using standard lock-in techniques.

## IV. RESULTS AND DISCUSSION

A PL spectrum of each sample recorded at $T = 2$ K is presented in Fig. 1. It can be seen that each spectrum shows an intense broadband (full width at half maximum ~90 meV), located below the fundamental GaAs band gap, and a very weak emission (around 1.519 eV) originating from the undoped GaAs host material. As we shall show later, a detailed analysis of the PL spectra as a function of temperature indicated that this broadband consisted of several emission peaks. Our set of samples, S500, S300, S250, and S200 behaved in the same qualitative way and exhibited the characteristics of isolated $\delta$-doped wells, whereas S100 had a typical superlattice behavior. So, in the rest of the present work, we shall mainly discuss the results from samples S500 and S100.

The PL spectra of sample S500 recorded at different temperatures are shown in Fig. 2. Each PL spectrum was normalized to unity with respect to its most intense emission peak. It can be observed that, with increasing temperature, the intensity of the broadband decreases drastically with respect to the emission near the GaAs band gap, which becomes the dominant feature at $T > 80$ K. In order to understand the temperature behavior of the broadband, all the PL spectra were decomposed into their constituents, and their energies were plotted as a function of temperature as shown in Fig. 3(a) for sample S500. A schematic representation of the transitions obtained by the decomposition of the PL spectra is presented in Fig. 3(b). Good fits to the PL spectra were obtained when the broadband was weighted towards a linear superposition of Gaussian curves, whereas the emission near the GaAs band gap was adjusted by a Lorentzian curve. Representative PL spectra obtained with our line-shape analysis are shown in Fig. 4 for sample S500 at two different temperatures. At $T = 2$ K, the highest-energy peak resulting from the decomposition of the broadband was a free-to-bound (FB) transition, around 1.485 eV, involving $Si_{As}$ acceptors.[23]

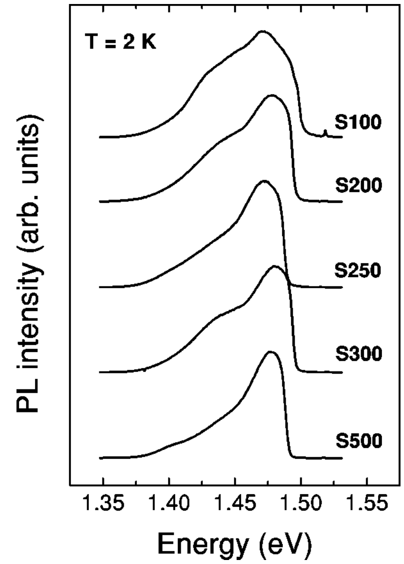


FIG. 1. 2 K PL spectra of multiple $p$-type $\delta$-doped GaAs layers with a fixed nominal sheet concentration in the $\delta$-doped layers ($N_A = 1.5\times10^{13}$ cm$^{-2}$) and different doping periods $d$ ranging from 100 to 500 Å.

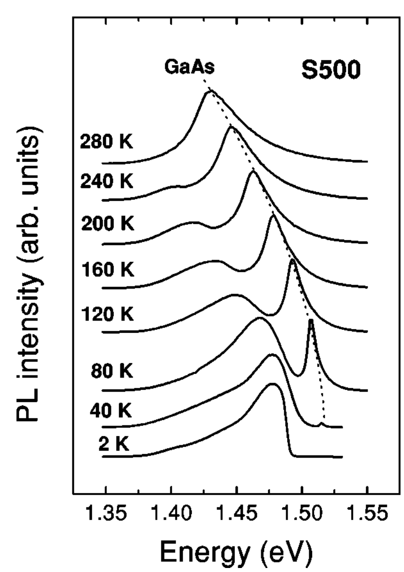


FIG. 2. PL spectra of sample S500 as a function of temperature.

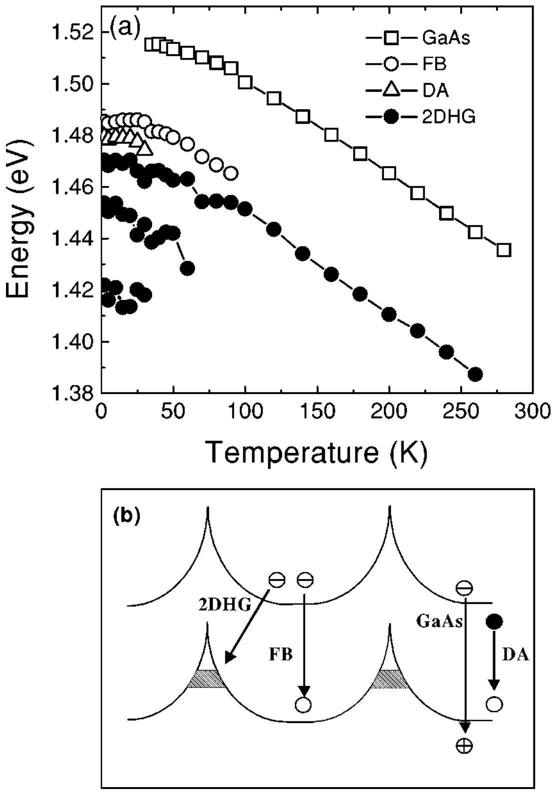


FIG. 3. (a) Energy chart of the peaks constituting the PL spectra of S500 as a function of temperature. The decomposition was realized as shown in Fig. 4 and explained in the text. The open squares are related to the band-to-band GaAs recombination and the open circles and triangles are related to the FB and DA transitions, respectively. The filled circles are emissions related to the 2DHG. The lines connecting the points are only a guide to the eyes. (b) Schematic representation of the transitions taking place in S500.

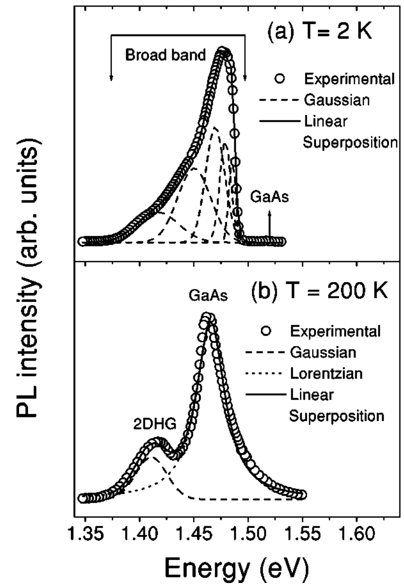


FIG. 4. Representative decomposition of the PL spectra obtained with our line-shape analysis for sample S500 at two different temperatures: (a) $T=2$ K; (b) $T=200$ K. The open circles are the experimental data and the solid line represents the linear superposition of the fitted peaks. The vertical arrow in (a) indicates the energy position of the weak GaAs emission.

Another peak was obtained around 1.479 eV and is probably related to a donor-acceptor (DA) transition involving a $Si_{Ga}$-$Si_{As}$ pair.[23] Besides these two extrinsic emissions originating from the undoped host material, our fitting procedure also indicated the presence of three peaks around 1.468 eV, 1.454 eV, and 1.421 eV (denoted in our paper as 2DHG bands), which were ascribed to the radiative recombination of photogenerated electrons with the confined holes of the 2DHG. Though there exist several different ways to decompose the broadband of our optical data, the physical meaning of our findings indicated that our fitting procedure provided a reliable description of the emissions observed in the PL spectra as a function of temperature. It is important to emphasize that the 2DHG bands obtained by the line-shape analysis of the PL spectra are not necessarily related to the subband structure of M$\delta$D GaAs layers. Broad structureless emission spectra have already been observed by other groups investigating M$\delta$D GaAs layers,[8–11] but only two of them reported emissions related to the confined states associated to the electronic subband structure for *n*-type M$\delta$D GaAs layers with $\delta$ planes separated by 500 Å in Ref. 10 or 350 Å in Ref. 11.

The space-charge potential in M$\delta$D layers modulates the band edges of the host material in such a way that majority and minority carriers become spatially separated. In widely spaced *p*-type M$\delta$D layers (as for S500), the majority carriers (holes) are confined along the growth direction by the ''$\Lambda$''-shaped potential well induced by the $\delta$-doped planes, while the minority carriers (photogenerated electrons) are in the conduction band in confined states of the potential wells located between adjacent $\delta$-doped planes. Therefore, in the active region of widely spaced M$\delta$D layers, two channels are available for the radiative recombination of photoexcited minority carriers: the channel associated to the 2DHG and the one related to background impurities and free holes from the undoped GaAs region between adjacent $\delta$-doped layers. Depending on the temperature range, one of these channels will dominate the process of radiative recombination of the photogenerated electrons. At sufficiently low temperature, the $\delta$-doped wells are attractive for the photogenerated free holes. They will be captured by the $\delta$ wells and the main recombination paths in the active region will be through the 2DHG and the background impurities. Therefore, the capture of free holes photocreated in the GaAs host material located between adjacent $\delta$-doped planes leads to the weak emission near the GaAs band gap (around 1.519 eV). When the sample temperature is raised, the capture process of photogenerated holes is no longer efficient. Moreover, due to the escape of the holes from the $\delta$ wells and due to the thermal ionization of the $Si_{Ga}$ donor and $Si_{As}$ acceptor impurities (see the behavior of the DA and FB transitions in Fig. 3), the band-to-band recombination between holes and electrons in the undoped GaAs regions between adjacent $\delta$-doped layers becomes the dominant recombination path. Summarizing, at low temperature, the broadband consists of the superposition of emissions resulting from the radiative recombination of photogenerated electrons and holes of the 2DHG (leading to the 2DHG bands) and also background impurities located between $\delta$-doped planes (leading to the FB and DA emission peaks). At higher temperature, the remaining broadband is mainly related to the weak radiative recombination involving

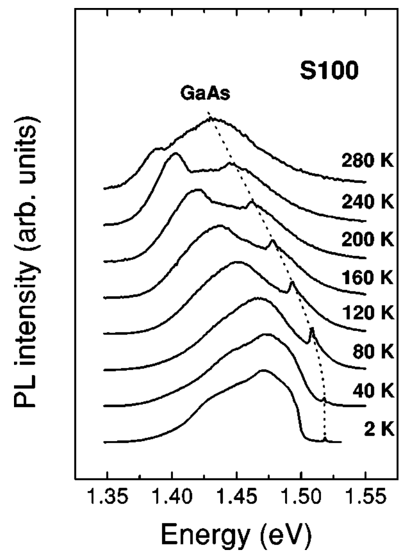


FIG. 5. PL spectra of sample S100 as a function of temperature.

the holes of the 2DHG. The dominant emission is the band-to-band recombination involving holes in the undoped GaAs regions between $\delta$-doped planes originating from the thermal ionization of background impurities and from the efficient escape of the holes from the 2DHG.

For sample S100, unlike the other samples of the set, the weak peak observed at low temperature near the GaAs band edge does not become the dominant recombination path, as can be observed in the PL spectra of Fig. 5. At high temperature, the intensity of the 2DHG band is of the same order as that of the GaAs emission, and both of them have the weakest luminescence signal when compared with all the other samples, as can be observed in Fig. 6(a), where we showed the maximum absolute intensity of the emission near the GaAs band edge as a function of temperature for some of the samples. It can be noticed in this figure that the intensities reach a maximum around 100 K for the samples with the largest periods, whereas the intensity of the GaAs peak of sample S100 is only weakly dependent on temperature. Another important feature, which can be noted in Fig. 6(a), is that the GaAs emission becomes less intense as the period of the M$\delta$D structure decreases. As already discussed, for the samples with the largest periods the observed intensity enhancement is due to the thermal activation (escape) of the holes from the $\delta$-potential wells to the nearby GaAs regions between the $\delta$-doped planes and the thermal ionization process of the background impurities. Beyond 100 K, the intensity decreases because nonradiative processes are more pronounced at higher temperature. In M$\delta$D structures with a large period, the overlap between the wave functions of the holes of the 2DHG and the photogenerated electrons is reduced. As a result, longer radiative lifetimes associated to the radiative recombination process of the 2DHG are expected as compared to the direct recombination process occurring in the GaAs regions between $\delta$-doped planes. That is the reason why at high temperature, when there are available free holes for direct recombination, the GaAs band-to-band recombination becomes the dominant emission in the PL spectra as compared to the 2DHG-emission band. When the period is made shorter, but the $\delta$ wells are still considered as isolated, the wave-function overlap will gradually be larger and larger, leading to an increase of the 2DHG optical-recombination probability to the detriment of the recombination probability inside the GaAs regions. This explains why at a fixed temperature in the range 40 K $< T <$ 100 K, the GaAs emission is less intense for the samples with smaller and smaller doping periods as observed in Fig. 6(a). When the period is further reduced, the system experiences a 2D to 3D transition, where minibands are formed and the wave functions of majority and minority carriers are spread out along the whole periodic structure. Consequently, the intensity of the 2DHG band should first increase, reaching a maximum for a critical period, and then should drop as the period is further reduced, as already observed in *n*-type M$\delta$D layers.[12] According to this, it seems that sample S100 has a predominant 3D character and the observed emission near the GaAs band gap should be originating from the GaAs buffer layer since the recombination paths associated with the GaAs regions between $\delta$-doped planes were suppressed.

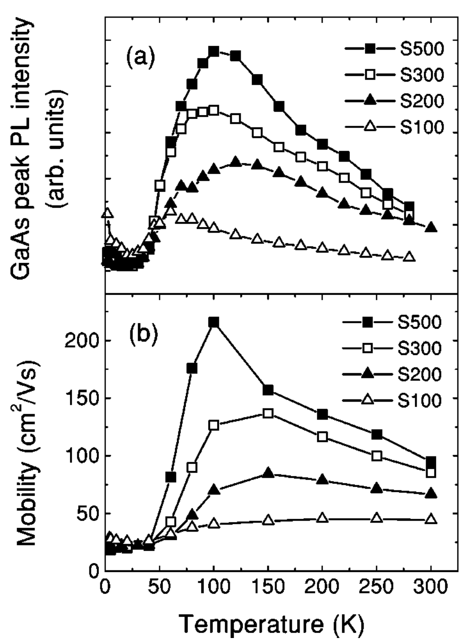


FIG. 6. Temperature dependence: (a) of the absolute maximum intensity of the emission near the GaAs band edge and (b) of the Hall mobility for samples S500, S300, S200, and S100. The lines connecting the points are only a guide to the eyes.

The influence of the escape of the holes from the $\delta$-potential wells on the electrical properties is shown in Fig. 6(b) where the temperature dependence of the Hall mobility ($\mu_{\mathrm{Hall}}$) is presented for some of the samples. In the temperature range from 2 up to 40 K, the value of the Hall mobility is roughly the same for all the samples. With the exception of sample S100, we can observe that the Hall mobility increases monotonically with raising temperatures in the range 40 K $< T <$ 100 K and this variation is more pronounced for the structures with the largest periods. Beyond 100 K, the mobility decreases as a consequence of scattering by optical phonons. We can conclude, from the compelling correlation between the optical and electrical measurements presented here, that the mobility enhancement is also due to the escape of holes from the $\delta$ wells. In the following, we shall explain the correlation between the escape of holes and the observed enhancement of $\mu_{\mathrm{Hall}}$ with increasing temperature that suggests some form of hole scattering by ionized impurities.

Considering that the undoped GaAs regions between $\delta$ wells have a low impurity-background level with respect to the dopant concentration in the planar layers, we shall neglect in the present discussion the effects of Coulombic scattering due to background ionized impurities. So, only scattering events involving holes and ionized dopant atoms from the $\delta$-doped layers will be taken into account. According to the two-carrier conduction theory, two types of holes can be responsible for the mobility enhancement: (i) the holes which escaped from the $\delta$ wells and (ii) the holes which remained confined in the $\delta$ wells. Let us first discuss the effects of the escape of holes on the mobility of the 2DHG. Self-consistent calculations showed[17–19] that the Fermi level in $p$-type $\delta$-doped GaAs layers was always located inside the $\delta$-potential well, differently from the Fermi level in $n$-type $\delta$-doped GaAs layers, which was always very close to the continuum states of the GaAs conduction band. The same calculations pointed out that the Fermi level was located deeper and deeper inside the $\delta$ well when the distance between them was made larger. Thus, for a given temperature, the escape rate of the holes from the $\delta$ wells will be smaller for the structures with the largest periods as a consequence of their higher escape activation energies. For instance, for M$\delta$D structures with $N_A = 1.5\times 10^{13}\ \mathrm{cm}^{-2}$ and doping periods $d$ in the range 100 Å$\leqslant d \leqslant$500 Å, the Fermi level is located approximately 20 meV below the continuum states of the GaAs valence band.[19] As a result, an efficient thermal activation of holes from the $\delta$ wells to the nearby GaAs regions is expected in $p$-type M$\delta$D systems. Before concluding this analysis, we should point out that the calculations mentioned here refer to M$\delta$D structures grown in the [100] direction since there have been no theoretical results published for these systems grown in the [311] direction so far. However, preliminarly calculations for an isolated $p$-type $\delta$-doped GaAs well grown along the [311] axis revealed that the Fermi level is even shallower than that obtained for the $\delta$ well grown in the [100] direction with the same acceptor concentration.[24]

The scattering by ionized impurities in degenerated 2D doped semiconductors cannot be expressed in a closed form as is the case in conventional nondegenerated 3D doped samples that follow the Brooks-Herring expression.[25] However, in our case we can assume that, in the temperature range where scattering by ionized impurities dominates the conduction process, the mobility can be described by the equation[26]

$$\mu_{\mathrm{Hall}}(T) = \frac{f(T,p)}{N_I(T)}, \tag{1}$$

where $f(T,p)$ is a function of temperature $T$ and of the concentration $p$ of the 2DHG, and $N_I(T)$ represents the 2D concentration of ionized impurity atoms in the $\delta$-doped layers. The periodic space-charge potential, which modulates the band edges along the growth direction, is generated by the balance of the ionized impurities of the $\delta$ layer and the carriers of the 2DHG. The escape of holes from the $\delta$-potential wells leads to a non-fully-compensated $\delta$-doped layer, increasing the average number of scattering centers due to the partial screening of the ionized donors of the $\delta$-doped layers. The phenomenological relation (1) expresses the fact that the mobility of the confined holes should drop with the increasing number of ionized scattering centers $N_I(T)$. Thus, we can deduce that for a given temperature, the mobility will be higher for the structures with the largest periods, which is in good agreement with our experimental observations. This interpretation is based on the assumption that $f(T,p)$ does not change too much with temperature from sample to sample, i.e., the variation of the concentration of confined holes as a function of temperature has a minor effect on the mobility of the 2DHG, and on the fact that $N_I(T)$ has a weaker temperature dependence when the period of the M$\delta$D structure is made larger (as mentioned before, the Fermi level is located deep inside the $\delta$ well for the structures with the largest periods).

The same analysis is useful to describe the mobility behavior of the holes that escaped from the $\delta$-doped wells. In this case, a similar situation to modulation-doped quantum wells (MDQWs) takes place: the mobile carriers are spatially separated from their ionized parent impurities located in the $\delta$-doped planes. However, differently from our samples, in MDQWs, the scattering of carriers from the ionized dopant atoms is negligible and the low-temperature dependence of the mobility is mainly determined by acoustic-phonon scattering.[27] So, in M$\delta$D structures, the Coulombic interaction of the holes that escaped from the $\delta$ wells with the ionized dopant atoms in the non-fully-compensated $\delta$-doped layers should also be taken into account in the analysis of the observed mobility enhancement.

To finalize the presentation of our results, it important to say that the structure with the smallest period exhibits obvious superlattice behavior: very low PL intensity related to the recombination of photogenerated electrons and holes of the 2DHG, and weak temperature dependence of the mobility with temperature.

## V. CONCLUSION

The electrical and optical characteristics of multiple $p$-type $\delta$-doped GaAs (311)$A$ layers with a fixed nominal sheet concentration and different doping periods have been investigated as a function of temperature. An enhancement of the Hall mobility for the structures with the highest periods as compared to the mobility of structure with the smallest period was observed and attributed to the escape of holes of the 2DHG from the $\delta$ wells. It is, however, clear that a full quantitative treatment to describe the observed data requires a self-consistent calculation of the hole transport in $\delta$-doped $p$-type GaAs layers that includes the effect of the escape of holes from the $\delta$ wells in the electronic structure of the system.

[1] E. F. Schubert, *Semiconductors and Semimetals*, edited by Arthur C. Gossard (Academic, New York, 1994), Vol. 40, p. 1.
[2] For a recent and complete review, see *Delta-doping of Semiconductors*, edited by E. F. Schubert (Cambridge University Press, Cambridge, 1996).
[3] C. H. Perry, K. S. Lee, W. Zhou, J. M. Worlock, A. Zrener, F. Koch, and K. Ploog, Surf. Sci. **196**, 677 (1988).
[4] A. Levine, E. C. F. da Silva, G. M. Sipahi, A. A. Quivy, L. M. R. Scolfaro, J. R. Leite, I. F. L. Dias, E. Lauretto, J. B. B. de Oliveira, E. A. Meneses, and A. G. Oliveira, Phys. Rev. B **59**, 4634 (1999).
[5] I. A. Buyanova, W. M. Chen, A. Henry, W.-X Ni, G. V. Hansson, and B. Monemar, Phys. Rev. B **53**, 9587 (1996).
[6] X. Zheng, T. K. Carns, K. L. Wang, and B. Wu, Appl. Phys. Lett. **62**, 504 (1993).
[7] V. L. Gurtovoi, V. V. Valyaev, S. Yu. Shapoval, and A. N. Pustovit, Appl. Phys. Lett. **72**, 1202 (1998).
[8] S. M. Shibli, L. M. R. Scolfaro, J. R. Leite, C. A. C. Mendonça, F. Plentz, and E. A. Meneses, Appl. Phys. Lett. **60**, 2895 (1992).
[9] L. P. Sadwick, E. H. Reihlen, D. H. Jaw, R. J. Hwu, and D. C. Streit, J. Vac. Sci. Technol. B **11**, 120 (1993).
[10] A. J. Dewdney, S. Holmes, H. Yu, M. Fahy, and R. Murray, Superlattices Microstruct. **14**, 205 (1993).
[11] M. L. Ke, J. S. Rimmer, B. Hamilton, M. Missous, B. Khamsehpour, J. H. Evans, K. E. Singer, and P. Zalm, Surf. Sci. **267**, 65 (1992).
[12] P. L. Sousa, B. Yavich, M. Pamplona-Pires, A. B. Henriques, and L. C. D. Gonçalvez, J. Appl. Phys. **82**, 1700 (1997).
[13] H.-J Gossmann and F. C. Unterwald, Phys. Rev. B **47**, 12 618 (1993).
[14] A. B. Henriques, L. C. D. Gonçalves, N. F. Oliveira, Jr., P. L. Souza, and B. Yavich, Phys. Rev. B **55**, 13 072 (1997).
[15] C. A. C. Mendonça, F. Plentz, J. B. B. Oliveira, E. A. Meneses, L. M. R. Scolfaro, D. Beliaev, S. M. Shibli, and J. R. Leite, Phys. Rev. B **48**, 12 316 (1993).
[16] L. M. R. Scolfaro, J. R. Leite, C. A. C. Mendonça, D. Beliaev, S. M. Shibli, E. C. F. da Silva, and E. A. Meneses, Mater. Sci. Forum **143-147**, 669 (1994).
[17] G. M. Sipahi, R. Enderlein, L. M. R. Scolfaro, J. R. Leite, E. C. F. da Silva, and A. Levine, Phys. Rev. B **57**, 9168 (1998).
[18] G. M. Sipahi, R. Enderlein, L. M. R. Scolfaro, and J. R. Leite, Phys. Rev. B **53**, 9930 (1996).
[19] L. E. Ramos, G. M. Sipahi, L. M. R. Scolfaro, R. Enderlein, and J. R. Leite, Superlattices Microstruct. **22**, 443 (1997).
[20] L. M. Gaggero-Sager and R. Perez-Alvarez, Appl. Phys. Lett. **70**, 212 (1997).
[21] K. Agawa, K. Hirakawa, N. Sakamoto, Y. Hashimoto, and T. Ikoma, Appl. Phys. Lett. **65**, 1171 (1994).
[22] A. A. Quivy, M. Frizzarini, E. C. F. da Silva, A. L. Sperandio, and J. R. Leite, Braz. J. Phys. **27/A**, 125 (1997).
[23] M. Ilegens, in *The Technology and Physics of Molecular Beam Epitaxy*, edited by E. H. C. Parker (Plenum Press, New York, 1985), p. 98.
[24] G. M. Sipahi, private communication.
[25] Models for ionized impurity scattering were reviewed by D. Chattopadhyay and H. J. Queisser, Rev. Mod. Phys. **53**, 745 (1981).
[26] Jasprit Singh, in *Physics of Semiconductors and Their Heterostructures* (McGraw-Hill, New York, 1993), p. 359.
[27] For a review about MDQWs, see C. Weisbuch, *Semiconductors and Semimetals*, edited by R. Dingle (Academic, New York, 1987), Vol. 24, p. 78.